17th IMACS World Congress on Scientific Computation, Applied Mathematics and Simulation
Paris, France, 11–15 July 2005.

Construction of an A-switching Map to Control Nonlinear Dynamics of Electronic Converters

Cristina MOREL, Marc BOURCERIE, François CHAPEAU-BLONDEAU
Laboratoire d'Ingénierie des Systèmes Automatisés (LISA), CNRS FRE 2656, Université d'Angers,
62, Avenue Notre Dame du Lac 49000 Angers, France
Phone: +33.2.41.22.65.60, Fax: +33.2.41.22.65.61, E-mail: cristina.morel@univ-angers.fr

Abstract - In this paper, nonlinear phenomena appearing in DC-DC converters are analyzed by using a discrete time nonlinear map (the A-switching map). We then propose a feedback control method improving switch-mode power supplies electromagnetic compatibility (spectral peaks compliance). To confirm the efficiency of this new and simple method, the map is derived in closed form from the system of nonlinear equations of a Buck converter.

Keywords—**anticontrol of chaos, Buck converter, power spectrum, output voltage ripple, A-switching map.**

I. INTRODUCTION

DC-DC converters are widely used power electronics circuits. They stabilize a DC voltage to a higher (Boost), a lower (Buck) or a generic (Buck-Boost) value. This is usually performed by pulse width modulating the input voltage.

These converters' rapid switchings of high currents and high voltages generate electromagnetic interference which create significant difficulties to comply with new regulations [DEA 99]. Various methods of interference emission reduction, by modulating the switching frequency of power supplies, have been proposed, enabling to modify noise emission spectrum [LIN 94] [STA 95].

Chaos, a phenomenon occurring in DC-DC converters (switch-mode power supplies), might help reducing spectral peaks [DEA 96] [DEA 99]; the usual goal has long been its suppression (chaos control) [MOR 00] [MOR 02], i.e. the transition between chaos to order. We are now interested in studying the transition between order to chaos [MOR 04] [MOR 05], sometimes called chaotification or anticontrol of chaos.

The application of chaos anticontrol [CHE 97] [WAN 01] to switch-mode power supplies leads the output voltage to have an exaggerated output voltage ripple or an undesirable spectrum [CHA 97] [WOY 03]. This is why we propose here a simple feedback control method.

Finally, a two-dimensional A-switching map describing the behavior of the controlled Buck converter is calculated (including a new case of map impact) [BER 98] and [BER 00]. This map is necessary to determine the power spectrum of the output voltage and to ensure that our controller improves the electromagnetic compatibility and eliminates the previous drawbacks.

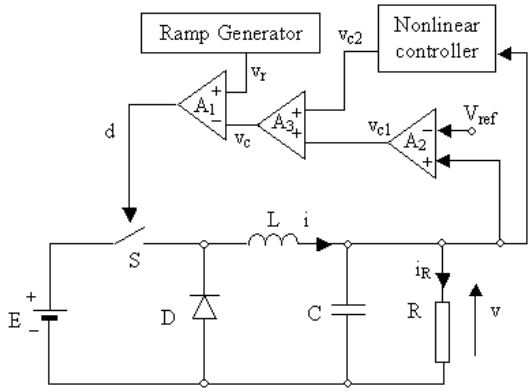

Fig. 1. DC-DC Buck converter with feedback controls. The nominal values of the fixed parameters are: $L = 20\,\text{mH}$, $C = 47\,\mu\text{F}$, $R = 22\,\Omega$, $a = 8.4$, $V_{ref} = 11.3\,\text{V}$, $V_L = 3.8\,\text{V}$, $V_U = 8.2\,\text{V}$, $T = 400\,\mu\text{s}$ and $E = 16\,\text{V}$.

II. THE BUCK CONVERTER

Fig. 1 shows the block diagram of a Buck converter that uses a pulse width modulation voltage loop [FOS 96]. The circuit has two states: when the switch S is (either) closed or open. When S is closed, the input E provides energy to the load R as well as to the inductor L. When S is open, the inductor current, which flows through the diode D, transfers some of its stored energy to the load R. The amplifier A_2 has a gain a. The most general and simplest form of feedback of the converter is using the potentiometer P in the zero position (Fig. 1). In this way, the control voltage $v_c(t)$ can be written as

$$v_c(t) = v_{c1}(t) = a(v(t) - V_{ref}). \tag{1}$$

The control voltage $v_c(t)$ is applied to the inverting input of the comparator A_1. The non-inverting input is connected to an independently voltage ramp generater, which periodically rises from a low voltage V_L to an upper voltage V_U in a time T, and then instantaneously returns to V_L. The ramp voltage can be expressed as:

$$v_r(t) = V_L + (V_U - V_L)\frac{t \bmod T}{T}. \tag{2}$$

The switch S is open (and diode D conducts) when $v_c(t) \geq v_r(t)$; otherwise S is closed (and D is blocked).

The systems is governed by two sets of linear differential equations pertaining to the on and off states of the controlled switch. The voltage $v(t)$ of the capacitor C and the inductance current $i(t)$ are taken as state variables [HAM 92].
The dynamic model can be written as

$$\frac{dv}{dt} = -\frac{1}{C}i(t) - \frac{1}{RC}v(t), \tag{3}$$

$$\frac{di}{dt} = -\frac{1}{L}v(t) + \frac{E}{L}d(t), \tag{4}$$

where E is a constant input voltage, and $d(t)$ the modulated signal which is zero when $v_c(t) \geq v_r(t)$ and one when $v_c(t) < v_r(t)$. If we fix a set of initial conditions $v_0 = v(t_0)$, $i_0 = i(t_0)$ and t_0=0, as the differential equations are linear, the solutions of the system can be determined:

$$v(t) = e^{-kt}\left[v_0\cos(\omega t) + \left(\frac{i_0}{\omega C} - \frac{kv_0}{\omega}\right)\sin(\omega t)\right] \tag{5}$$

$$i(t) = e^{-kt}\left[i_0\cos(\omega t) + \left(\frac{ki_0}{\omega} - \frac{v_0}{\omega L}\right)\sin(\omega t)\right] \tag{6}$$

if $v_c(t) \geq v_r(t)$. For the other case ($v_c(t) < v_r(t)$), the solutions are:

$$\begin{aligned} v(t) &= E + e^{-kt}(v_0 - E)\cos(\omega t) \\ &\quad + e^{-kt}\left(\frac{i_0 - \frac{E}{R}}{\omega C} - \frac{k(v_0 - E)}{\omega}\right)\sin(\omega t), \end{aligned} \tag{7}$$

$$\begin{aligned} i(t) &= \frac{E}{R} + e^{-kt}\left(i_0 - \frac{E}{R}\right)\cos(\omega t) \\ &\quad + e^{-kt}\left(k\frac{i_0 - \frac{E}{R}}{\omega} - \frac{v_0 - E}{\omega L}\right)\sin(\omega t), \end{aligned} \tag{8}$$

with $k = \frac{1}{2RC}$ and $\omega = \sqrt{\frac{1}{LC} - k^2}$ (we assume that $\frac{1}{LC} - k^2 > 0$). Elementary converters are second-order systems since they have two energy storage elements. Therefore, for any given switch condition, two first-order differential equations are required to describe the total behavior of the system. For DC-DC converters, the switching time depends nonlinearly on the history of the state variables: the system is effectively nonlinear. Hence, this kind of piecewise model, at least in principle, satisfies the requirements for chaos.
In general, these circuits produce an average DC output voltage with periodic ripples (70mV Fig. 2). Fig. 3 represents the power spectrum of the output voltage $v(t)$ when

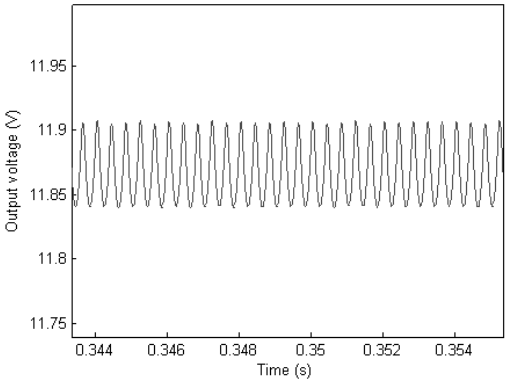

Fig. 2. Time-domain waveform of the output voltage Buck converter: fundamental periodic operation.

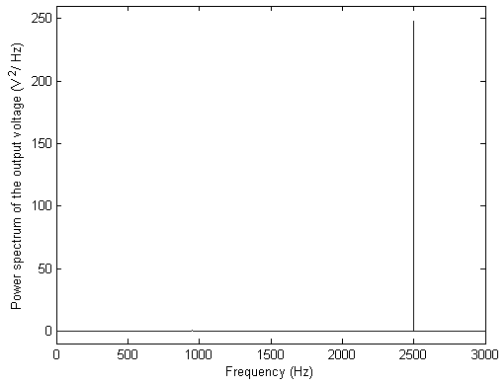

Fig. 3. Power spectrum of the output voltage $v(t)$ for the circuit (1).

the converter is governed by the control law $v_{c1}(t)$ of Eq. (1). The spectrum has a peak at the switching frequency $1/T$, with a magnitude of $250\,\mathrm{V}^2/\mathrm{Hz}$.
For the electromagnetic compatibility compliance reasons, let us try to reduce the peak value of the spectrum while maintaining a small ripple. Chaotifying a system supposes to design a nonlinear controller $c_2 \sin[\omega_2(v(t) - V_{ref})]$, with a small amplitude c_2 such that the non-chaotic dynamical system becomes chaotic [WAN 01] [CHE 97]. The application of this method to switch-mode power supplies leads the output voltage $v(t)$ to have an exaggerated output voltage ripple (i.e. with regards to electromagnetic compatibility compliance) [CHA 97] [WOY 03]. Unfortunately, this study with the classical method disables to choose the coefficient c_2 and the angular pulsation ω_2 because of the large ripple, which reduces the efficiency of the DC-DC converter [MOR 04]. Even if many other spectral lines appear, on the process of chaotifying the system, the output voltage ripple influences the amplitude of the power spectral density.
One can wonder why we need to apply a method to generate chaos, when chaos is a phenomenon which can occur naturally in switch-mode power supplies [FOS 96]. The Buck converter is characterized by a chaotic behavior for

the input voltage E superior to 32.34V, governed by the control law (1). The case is not acceptable also because of a higher ripple [FOS 96] [BER 98] than in the previous case. This is why we need to find another solution.

III. BOUNDING THE OUTPUT VOLTAGE RIPPLE

We introduce a new nonlinear controller, with the only target to obtain an output voltage $v(t)$ with power spectrum and ripple smaller than the converter is governed by the control law (1). We proposed the new control law:

$$v_c(t) = v_{c1}(t) + v_{c2}(t) \tag{9}$$

where:

$$v_{c2}(t) = c_3 v(t) \sin(\omega_3 t) = c_3 v(t) \sin(2\pi f_3 t). \tag{10}$$

is the new nonlinear controller proposed in this paper. This time the expression (10) includes multiplication of the feedback state converter and a sinus. The amplitude and frequency of v_{c2} influence the number of switchings. Furthermore, S switches many times during one period of the ramp (Fig. 4), if for this nonlinear controller, we choose the frequency f_3 much greater than the frequency $(1/T)$ of the ramp generator. Because of these multiple switches, the output voltage does not have enough time to rise or to decrease too much.

Let us vary the pulsation ω_3 and the amplitude c_3, in order to find the best possible power spectrum and ripple. Choosing ω_3 is very simple: it must be much greater than the angular frequency $(2\pi/T)$ of the ramp generator and on the other way, the switching frequency of the switch S is limited to [80 kHz, 100 kHz], in practice. So, we can write:

$$\frac{2\pi}{T} \ll \omega_3 < 80\, kHz. \tag{11}$$

[MOR 04] and [MOR 05] show very clearly that high frequencies have no more influence on the ripple. Our choice is f_3 ≈40kHz.

The choice of coefficient c_3 could only be done to minimize the power spectrum.

IV. DESCRIPTION OF THE DYNAMIC SYSTEM BY A MAP

An iterative map consists in calculating the output voltage v, the inductance current i, or time t at the moment $m+1$ in function of the same variables at the moment m.

$$(v_m, i_m, t_m) \rightarrow (v_{m+1}, i_{m+1}, t_{m+1}). \tag{12}$$

Such a map, applied to the state space, will give the state of the system at an A-switching instant in terms of the previous one. The A-switching instants result from the intersection between the ramp voltage $v_r(t)$ and the control voltage $v_c(t)$ waveforms, rejecting the time instants multiple of

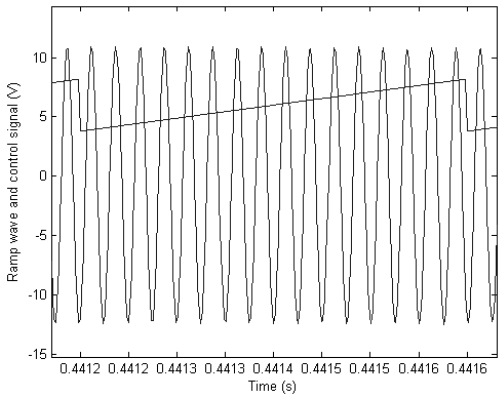

Fig. 4. Triangular wave $v_r(t)$ and control signal $v_c(t)$ for the circuit with the control laws (10) and (1).

ramp voltage period T, if they exist. The A-switching moments are defined by the equality of the control law (10) (1) and the ramp voltage $v_r(t)$:

$$a\,[v(t) - V_{ref}] + c_3 v(t) \sin(\omega_3 t) =$$

$$= V_L + \frac{V_U - V_L}{T}(t \bmod T). \tag{13}$$

We now detail how [BER 98] constructs the A-switching map. Let us indicate the solution of (5-6), from the A-switching instant t_m to the next one t_{m+1} as

$$v_{m+1} = e^{-k\Delta} v_m \cos(\omega\Delta) +$$

$$+ \quad e^{-k\Delta}\left(\frac{i_m}{\omega C} - \frac{k v_m}{\omega}\right)\sin(\omega\Delta), \tag{14}$$

$$i_{m+1} = e^{-k\Delta} i_m \cos(\omega\Delta) +$$

$$+ \quad e^{-k\Delta}\left(k\frac{i_m}{\omega} - \frac{v_m}{\omega L}\right)\sin(\omega\Delta). \tag{15}$$

The solutions of (7-8), between the instants t_m and t_{m+1} are:

$$v_{m+1} = E + e^{-k\Delta}\,(v_m - E)\cos(\omega\Delta) +$$

$$+ \quad e^{-k\Delta}\left(\frac{i_m - \frac{E}{R}}{\omega C} - \frac{k(v_m - E)}{\omega}\right)\sin(\omega\Delta), \tag{16}$$

$$i_{m+1} = \frac{E}{R} + e^{-k\Delta}\left(i_m - \frac{E}{R}\right)\cos(\omega\Delta) +$$

$$+ \quad e^{-k\Delta}\left(k\frac{i_m - \frac{E}{R}}{\omega} - \frac{v_m - E}{\omega L}\right)\sin(\omega\Delta), \tag{17}$$

where $\Delta = t_{m+1} - t_m$.

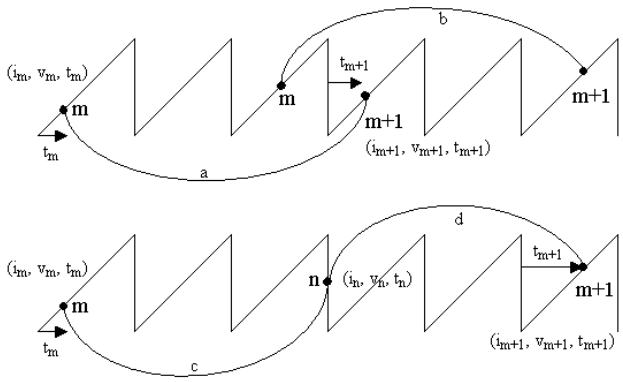

Fig. 5. Different typical behaviors of the control voltage between two A-switchings.

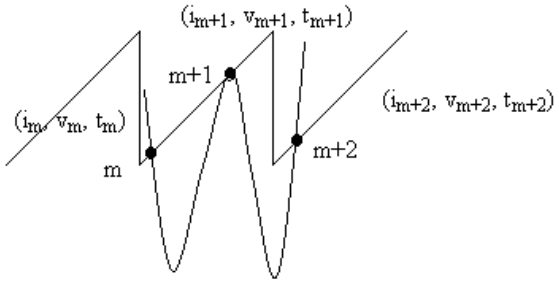

Fig. 6. New case of impact between two A-switchings.

Thus, we obtain the desired map, which can be written as:

$$\begin{cases} v_{m+1} = f_v(v_m, i_m, t_m, t_{m+1}) \\ i_{m+1} = f_i(v_m, i_m, t_m, t_{m+1}) \end{cases} \tag{18}$$

The explicit form (14), (16) or (15), (17) of the functions f_v and f_i depend on the voltage, current and time at the moment m and at the moment $m+1$. Since t_m and t_{m+1} are the A-switching instants, we can write:

$$v_m + \frac{c_3}{a} v_m \sin(\omega_3 t_m) = \alpha + \beta(t_m \bmod T) \tag{19}$$

$$v_{m+1} + \frac{c_3}{a} v_{m+1} \sin(\omega_3 t_{m+1}) = \alpha + \beta(t_{m+1} \bmod T) \tag{20}$$

which results (1-2) at each moment m. α and β have the following expressions

$$\alpha = V_{ref} + \frac{V_L}{a}, \qquad \beta = \frac{V_U - V_L}{aT}. \tag{21}$$

The explicit expression of v_m and v_{m+1} are reduced to the simplest form, function of time:

$$v_m = \frac{\alpha + \beta t_m \bmod T}{1 + \frac{c_3}{a}\sin(\omega_3 t_m)} = g(t_m), \tag{22}$$

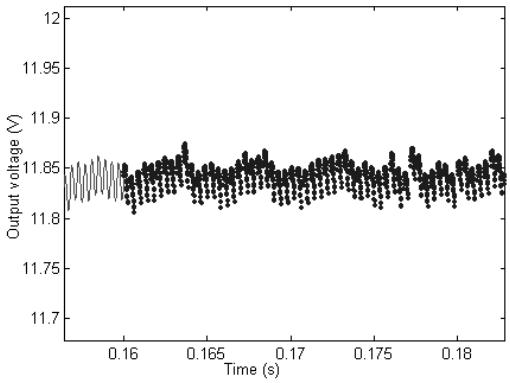

Fig. 7. Superposition of two output voltage waveforms issued from simulation and A-switching map for $c_3 = 0.2$.

$$v_{m+1} = \frac{\alpha + \beta t_{m+1} \bmod T}{1 + \frac{c_3}{a}\sin(\omega_3 t_{m+1})} = g(t_{m+1}). \tag{23}$$

Let us apply (22) to (18). i_{m+1} has the explicit form:

$$i_{m+1} = f_i(g(t_m), i_m, t_m, t_{m+1}) \tag{24}$$

For the moment t_{m+1}, the unknown v_{m+1} can be eliminated, using (22) (23) and (18):

$$g(t_{m+1}) = f_v(g(t_m), i_m, t_m, t_{m+1}). \tag{25}$$

So, (t_{m+1}, i_{m+1}) is calculated only using (t_m, i_m), and there is a direct mathematical relation given by (24) and (25) linking these two pairs. The closed-loop A-switching iterative bi-dimensional map can then be obtained, considering the pairs:

$$(t_m, i_m) \rightarrow (t_{m+1}, i_{m+1}). \tag{26}$$

With the value of t_{m+1}, we can calculate v_{m+1} using (18). The structure of f_v and f_i changes according to the two successive A-switchings [BER 00]. We need to identify these functions according to the desired map. Fig. 5 shows the trajectory of the system: the possible cases of the successive impacts a), b), c) and d).

Case a) (which corresponds to the ON phase) considers the relations (16) and (17). The expression of Δ is:

$$\Delta = t_{m+1} - t_m + s_{ON} \cdot T \tag{27}$$

where s_{ON} is the number of skipped cycles in the ON phase.

Case b) (valid for the OFF phase) considers the relations (14) and (15). The expression of Δ is:

$$\Delta = t_{m+1} - t_m + s_{OFF} \cdot T \tag{28}$$

where s_{OFF} is the number of skipped cycles in the OFF phase.

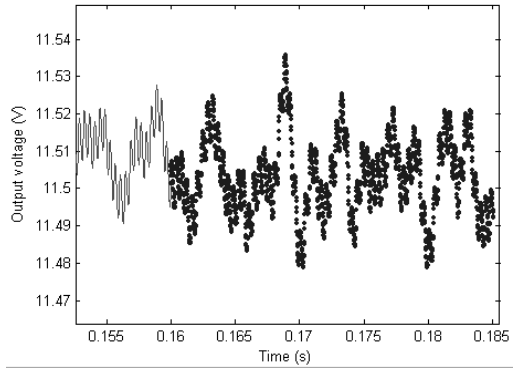

Fig. 8. Superposition of two output voltage waveforms issued from simulation and A-switching map for $c_3 = 0.6$.

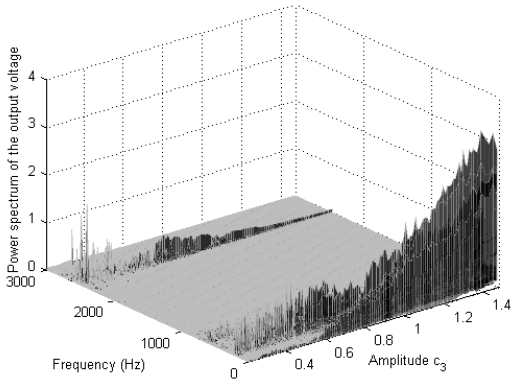

Fig. 9. Power spectrum with control laws (10) and (1) using the A-switching map.

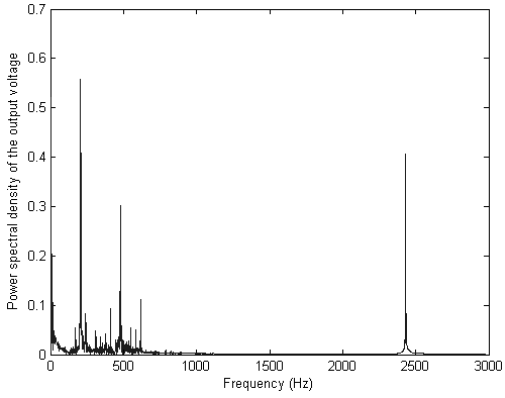

Fig. 10. Power spectrum of the output voltage obtained with c_3=0.71 using the A-switching map.

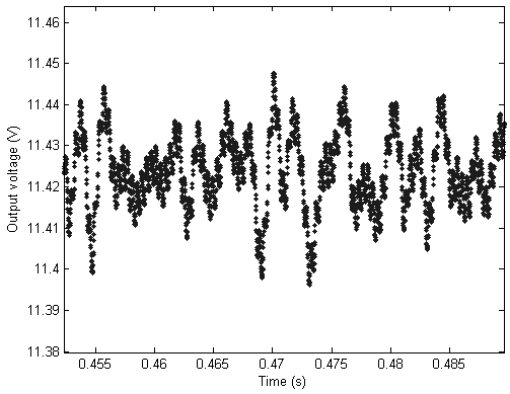

Fig. 11. Time wave-form of the output voltage obtained with c_3=0.71 using the A-switching map.

For the cases $c)$ and $d)$, we need to calculate the intermediary point n. For the ON phase, we apply the same relations (16) and (17), and obtain the pair (v_n, i_n). Then, the expression of Δ is:

$$\Delta = s_{ON} \cdot T - t_m. \tag{29}$$

For the last case, we apply (14) and (15), with the beginning point (v_n, i_n). Then:

$$\Delta = s_{OFF} \cdot T + t_{m+1}. \tag{30}$$

It is important to point out the presence of another case of impact (Fig. 6), where v_c is tangent to the ramp voltage. In this case, the expression (27) can be applied consecutively twice.

The discrete model enables one to avoid numerical computation of the phase space orbit from the continuous time model.

Fig. 7 and 8 show the time-domain waveform. This clearly show that the generated iterative map and the simulated wave-form have the same dynamics.

Fig. 9 shows the power spectrum (obtained as the Fourier transform of the autocorrelation) of the output voltage v_m, in function of c_3. The power contained in the peak of the switching frequency $1/T$ decreases when c_3 increases, whereas lower frequencies give high amplitudes of the power spectrum. The minimum value of the power spectrum amplitude is obtained for c_3=0.71. It represents the minimum of all the maxima of the power spectrum when c_3 varies.

Fig. 10 presents the power spectrum of the output voltage $v(t)$, for $c_3 = 0.71$ and $\omega_3 = 250000$ rad/s: min(maxFFT) is equal to $0.56\,\mathrm{V^2/Hz}$. We can observe that this spectrum is no more composed of a unique peak at the switching frequency $1/T$ (or at its harmonics): many spectral lines appear at lower frequencies, therefore widening the band.

Fig. 11 finally presents the temporal representation of the output voltage $v(t)$ and shows that the ripple is $55\,\mathrm{mV}$. Bifurcation diagram derived from the A-switching map in function of c_3 shown in Fig. 12.

The $v_{c2}(t)$ proposed here is introduced to maintain a small ripple of the output. Indeed, the two control laws $v_c(t) = v_{c1}(t)$ and $v_c(t) = v_{c1}(t) + v_{c2}(t)$ almost lead to the same ripple amplitude ($70\,\mathrm{mV}$, respectively $55\,\mathrm{mV}$). $v_{c2}(t)$, as system feedback, is able at the same time to reduce the power contained in the peaks of the switching harmonics of the DC-DC converter. We can say that $v_c(t) =$

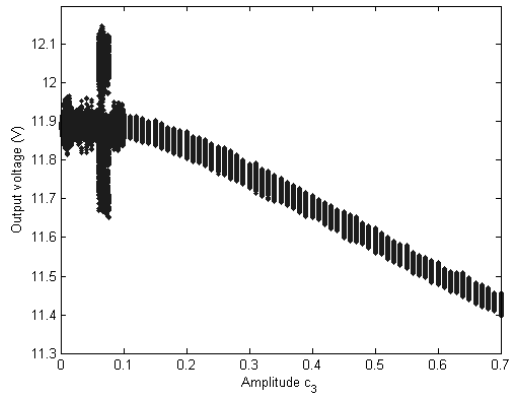

Fig. 12. Bifurcation diagram derived from the iterative map in function of c_3.

$v_{c1}(t)+v_{c2}(t)$ has better performances than $v_c(t) = v_{c1}(t)$. The new (non chaotical) nonlinear feedback controller improves the frequency-domain (spectrum) performance, without deteriorating the time-domain (ripple) performance.

V. CONCLUSION

We proposed an improvement of switch-mode power supplies electromagnetic compatibility by a feedback control method. The controller proposed in this paper improves the time-domain (ripple) performance and the frequency-domain (spectral) performance. Finally, a two-dimensional A-switching map describing the behavior of the controlled Buck converter is calculated (including a new case of map impact). This map is necessary to determine the power spectrum of the output voltage and to ensure that our controller improves the electromagnetic compatibility and eliminates the previous drawbacks (exaggerated output voltage ripple or undesirable spectrum).

REFERENCES

[BER 98] BERNARDO M. D., GAROFALO F., GLIELMO L., VASCA F., *Switchings, Bifurcations, and Chaos in DC-DC Converters*, *IEEE Transactions on Circuits and Systems I: Fundamental Theory and Application*, vol. 45, n2, p. 133–141, 1998.

[BER 00] BERNARDO M. D., VASCA F., *Discrete-Time Maps for the Analysis of Bifurcations and Chaos in DC-DC Converters*, *IEEE Transactions on Circuits and Systems I: Fundamental Theory and Application*, vol. 47, n2, p. 130–143, 2000.

[CHA 97] CHAN W. C. Y., TSE C. K., *Study of Bifurcations in Current-Programmed DC-DC Boost Converters: From Quasi-Periodicity to Period-Doubling*, *IEEE Transactions on Circuits and Systems -I: Fundamental Theory and Application*, vol. 44, n12, p. 1129–1142, 1997.

[CHE 97] CHEN G., LAI D., *Making a Dynamical System Chaotic: Feedback Control of Lyapunov Exponents for Discrete-time Dynamical Systems*, *IEEE Transactions on Circuits and Systems -I: Fundamental Theory and Application*, vol. 44, n3, p. 250–253, 1997.

[DEA 96] DEANE J. H. B., HAMILL D. C., *Improvement of Power Supply EMC by Chaos*, *Electronics Letter*, vol. 32, n12, p. 1045–1050, 1996.

[DEA 99] DEANE J. H. B., ASHWIN P., HAMILL D. C., JEFFERIES D. J., *Calculation of the Periodic Spectral Components in a Chaotic DC-DC Converter*, *IEEE Transactions on Circuits and Systems-I: Fundamental Theory and Application*, vol. 46, n11, p. 1313–1319, 1999.

[FOS 96] FOSSAS E., OLIVAR G., *Study of Chaos in the Buck Converter*, *IEEE Transactions on Circuits and Systems-I: Fundamental Theory and Application*, vol. 43, n1, p. 13–25, 1996.

[HAM 92] HAMILL D. C., DEANE J. H. B., JEFFERIES D. J., *Modeling of Chaotic DC-DC Converters by Iterated Nonlinear Mappings*, *IEEE Transactions on Power Electronics*, vol. 7, n1, p. 25–36, 1992.

[LIN 94] LIN F. L., CHEN D. Y., *Reduction of Power Supply EMI Emission by Switching Frequency Modulation*, *IEEE Transactions on Power Electronics*, vol. 9, n1, p. 132–137, 1994.

[MOR 00] MOREL C., Chaos in a Current-Mode Boost DC-DC Converter, *Online Symposium for Electronics Engineers OSEE 2000, USA*, n 290, 2000.

[MOR 02] MOREL C., Application of Slide Mode Control to a Current-Mode-Controlled Boost Converter, *Proceedings of the Annual Conference of the IEEE Industrial Electronics Society IECON'02, Sevilla, Spain*, p. 1824–1829, Nov 2002.

[MOR 04] MOREL C., BOURCERIE M., CHAPEAU-BLONDEAU F., Extension of Chaos Anticontrol Applied to the Improvement of Switch-Mode Power Supply Electromagnetic Compatibility, *Proceedings of the IEEE International Symposium on Industrial Electronics ISIE'04, Ajaccio, France*, p. 447–452, May 2004.

[MOR 05] MOREL C., BOURCERIE M., CHAPEAU-BLONDEAU F., *Improvement of Power Supply Electromagnetic Compability by Extension of Chaos Anticontrol*, *Journal of Circuits, Systems and Computers*, 2005 (accepted).

[STA 95] STANKOVIC A., VERGHESE G., PERREAULT D., *Analysis and Synthesis of Randomized Modulation Schemes for Power Converters*, *IEEE Transactions on Power Electronics*, vol. 10, n6, p. 680–693, 1995.

[WAN 01] WANG X. F., CHEN G., MAN K. F., *Making a Continuous-Time Minimum-Phase System Chaotic by using Time-Delay Feedback*, *IEEE Transactions on Circuits and Systems -I: Fundamental Theory and Application*, vol. 48, n5, p. 641–645, 2001.

[WOY 03] WOYWODE O., GULDNER H., BARANOVSKI A. L., SCHWARZ W., *Bifurcation and Statistical Analysis of DC-DC Converters*, *IEEE Transactions on Circuits and Systems-I: Fundamental Theory and Application*, vol. 50, n8, p. 1072–1080, 2003.